Pramana – J. Phys. (2016) 87: 56
DOI 10.1007/s12043-016-1264-0

Synthesis, characterization and third-order nonlinear optical properties of polydiacetylene nanostructures, silver nanoparticles and polydiacetylene–silver nanocomposites

B BHUSHAN[1,2,*], S S TALWAR[3], T KUNDU[1] and B P SINGH[1]

[1]Department of Physics, Indian Institute of Technology Bombay, Powai, Mumbai 400 076, India
[2]Present address: Department of Physics, Birla Institute of Technology, Mesra, Patna Campus, Near B V College, Patna 800 014, India
[3]Department of Chemistry, Indian Institute of Technology Bombay, Powai, Mumbai 400 076, India
*Corresponding author. E-mail: binaybhushan@gmail.com

MS received 1 July 2015; accepted 16 December 2015; published online 20 September 2016

Abstract. We have synthesized, characterized and studied the third-order nonlinear optical properties of two different nanostructures of polydiacetylene (PDA), PDA nanocrystals and PDA nanovesicles, along with silver nanoparticles-decorated PDA nanovesicles. The second molecular hyperpolarizability $\gamma(-\omega; \omega, -\omega, \omega)$ of the samples has been investigated by antiresonant ring interferometric nonlinear spectroscopic (ARINS) technique using femtosecond mode-locked Ti:sapphire laser in the spectral range of 720–820 nm. The observed spectral dispersion of γ has been explained in the framework of three-essential states model and a correlation between the electronic structure and optical nonlinearity of the samples has been established. The energy of two-photon state, transition dipole moments and linewidth of the transitions have been estimated. We have observed that the nonlinear optical properties of PDA nanocrystals and nanovesicles are different because of the influence of chain coupling effects facilitated by the chain packing geometry of the monomers. On the other hand, our investigation reveals that the spectral dispersion characteristic of γ for silver nanoparticles-coated PDA nanovesicles is qualitatively similar to that observed for the uncoated PDA nanovesicles but bears no resemblance to that observed in silver nanoparticles. The presence of silver nanoparticles increases the γ values of the coated nanovesicles slightly as compared to that of the uncoated nanovesicles, suggesting a definite but weak coupling between the free electrons of the metal nanoparticles and π electrons of the polymer in the composite system. Our comparative studies show that the arrangement of polymer chains in polydiacetylene nanocrystals is more favourable for higher nonlinearity.

Keywords. Polydiacetylene; nanoparticles; nanocomposites; hyperpolarizability.

PACS Nos 42.65.−k; 42.65.An; 42.70.Jk

1. Introduction

Considerable scientific research has been devoted to the development of efficient nonlinear optical materials for photonic devices such as ultrafast optical switching, optical data storage, optical limiting, modulators etc. For these devices, we need materials with high third-order susceptibility, low optical losses, fast response times, excellent optical transparency over wide spectral region, good processability and high chemical as well as optical stability. In this direction, conjugated organic polymers have emerged as potential materials because of the scope for judicious modifications of their basic molecular structure with the aim of enhancing both the polarizability as well as the anharmonicity of the electronic response. In the past, several strategies have been evolved to enhance the third-order nonlinear optical response of conjugated polymers like increasing the length of the conjugated systems, by substituting with conjugated rings, by polarizing the molecules with electron donor or acceptor substitution at the terminal position, introduction of quinoid character into the aromatic conjugated polymer backbone etc. However, according to the sum rule restricted three-level model by Kuzyk [1], there is a fundamental limit to the

second molecular hyperpolarizability (γ) shown by any molecule. Recent papers have reported the γ values approaching this fundamental limit by a factor of 2 [2] and 50 [3]. In spite of that, none of the existing conjugated polymers so far possesses the requisite figure-of-merit for the practical realization of all optical signal processing devices. The device-grade nonlinear optical polymers still remain a distant dream and new avenues are needed to be explored.

Among the varieties of conjugated polymers, polydiacetylenes (PDA) exhibit large potential for photonic device applications due to the ease of processability, variety of morphologies – crystalline or amorphous, large damage threshold and environmental as well as mechanical stability. Polydiacetylenes have been extensively explored for their nonlinear optical characteristics [4–8]. Apart from PDAs, metal nanoparticles have also been shown to exhibit large third-order nonlinearity $\{\chi^{(3)}\}$ and ultrafast response time [9–11]. A theoretical formalism for the third-order nonlinear optical response of the metal nanoparticles has been developed by Hache *et al* [12]. In a system of metal nanoparticles such as gold and silver dispersed in a transparent matrix, an absorption peak due to the surface plasmon resonance (SPR) is usually observed in the visible spectral region [13]. SPR is associated with the collective oscillation of free electrons of the metal nanoparticles which leads to the enhanced local electromagnetic fields. Due to the local field enhancement near the SPR, the third-order nonlinearity of the metal nanoparticles can be enhanced substantially. Silver nanoparticles have an advantage over other metal nanoparticles because the location of their surface plasmon resonance energy is quite far from the interband transition energy [14]. Therefore, in a sample containing silver nanoparticles embedded in a dielectric host, we can investigate the nonlinear optical effects focussing on the surface plasmon contribution. As both polydiacetylene as well as metal nanoparticles have been shown to exhibit considerable optical nonlinearity, it would then be very interesting to explore the nonlinear optical response of polydiacetylene–metal nanoparticle composite systems. Neeves and Birnboim [15], Kalyaniwalla *et al* [16] and Haus *et al* [17] have, in fact, theoretically predicted much larger enhancement of third-order nonlinearity of metallic shell-coated semiconductor arising from surface plasmon-enhanced local field. PDA–metal nanocomposites thus offer potential for enhanced nonlinear optical properties. However, optical nonlinearities of such composite systems have not been explored too much so far. More recently, some composites of PDA have been reported to have excellent nonlinear optical properties [18–21].

The samples which we have synthesized and characterized for investigating nonlinear optical properties are two different nanoassemblies of polydiacetylene, namely PDA nanocrystals and PDA nanovesicles, and also silver nanoparticles–PDA nanocomposites. The two nanoassemblies, by virtue of their basic structures, are expected to have differences in their chain packing geometry. Consequently, we have explored the influence of chain coupling effects facilitated by the chain packing geometry of PDAs on their third-order optical nonlinearity. Thereafter, the PDA nanovesicles were decorated by silver nanoparticles in order to understand the coupling between π electrons of the polymer and free electrons of the metal nanoparticles. The third-order nonlinear susceptibility of these samples has been investigated in the spectral range of 720–820 nm using transform-limited, 80 fs pulses (repetition rate = 100 MHz and energy per pulse = 5 nJ) from a self-mode-locked Ti:sapphire laser. We have used antiresonant ring interferometric nonlinear spectroscopic (ARINS) [22] technique to measure nonlinear optical response. As we have used femtosecond pulse and the ARINS set-up has been configured to measure nonlinearity faster than 3 ps (described below), the nonlinearity reported in this paper is purely of electronic origin. The subsequent spectral dispersion of second molecular hyperpolarizability has been analysed in the framework of three-essential states model and a correlation with the electronic structure of the samples has been discussed. The energy of the two-photon state, transition dipole moments and linewidth of the transitions have also been estimated. In order to compare the results of our nonlinear studies on silver–PDA nanocomposites, we have also synthesized, characterized and studied the nonlinear optical response of silver nanoparticles in aqueous solution.

2. Experimental details

2.1 *Synthesis and characterization of PDA nanovesicles and PDA nanocrystals*

A methodology for the preparation of polydiacetylene nanovesicles has been reported in [23]. But, in spite of our best efforts, we could not synthesize the same by adopting the reported procedure. Therefore, here we are reporting a slightly different method to synthesize PDA nanovesicles. The monomer used for the synthesis was high-purity diacetylene monocarboxylic acid, 10,12-pentacosadiynoic acid (PCDA), which was purchased from Alfa Aesar and used without further purification. First, we prepared an ethanol solution of the monomer having a concentration of 1.5×10^{-2} mol/l

in a test tube. The organic solvent was then rotaevaporated to give a thin film of the lipids on the glass surface of the test tube. Then, deionized water was added to yield typically a total lipid concentration of 1 mM. The resulting solution was filtered through a 1.2 μm filter and the filtrate was cooled at 4°C for 12 h. Polymerization was carried out at room temperature by irradiating the solution with 254 nm UV light (100 W) for 15 min to induce conjugated backbone of alternating double and triple bonds. Photopolymerization yielded a deep blue liquid containing the desired nanovesicles. A detailed explanation as well as schematic representation of the polymerization of diacetylene monomers and subsequent formation of nanovesicles has been given in [23,24].

For the synthesis of polydiacetylene nanocrystals, 2.5 ml of deionized water precooled to 20°C was taken in a 2 cm diameter test tube and stirred with a magnetic stirrer at a speed such that a whirlpool was formed. In this stirring state of water, 1.3 ml stock solution of 10,12-pentacosadiynoic acid (1.5×10^{-2} M) was added in the form of rapid stream using a syringe. This turned the solution milky. Next, the solution was sonicated for 20 min in an ultrasonic bath and then exposed to UV radiation for 15 min. Upon UV radiation, monomer nanoassemblies got polymerized to yield a deep blue solution containing PDA nanocrystals.

The two PDA nanostructures were characterized by UV–Vis absorption spectroscopy, transmission electron microscopy (TEM) and electron diffraction (ED). UV–Vis absorption spectra were taken with Jasco V-530 UV/Vis Spectrophotometer. The absorption spectra of PDA nanovesicles and nanocrystals are shown in figure 1. The absorption bands of π-conjugated polymeric diacetylene appear with vibronic peak at 631 nm and two secondary peaks at 582 nm and 542 nm respectively. The 542 nm peak corresponds to the vibronic peak which is seen in all polydiacetylenes. The origin of the peak at 582 nm could not be ascertained. It is our conjecture that it may be arising from the splitting of absorption peak due to the chain coupling. This can be confirmed by polarization studies which are not possible in solution and hence were not pursued further. Contrary to the three peaks shown by PDA nanovesicles, the UV–Vis absorption spectrum of PDA nanocrystals displays only two peaks at 664 nm and 582 nm. The second peak on the higher energy side is again a vibronic peak. Both the exciton and vibronic peaks in the PDA nanocrystals are red-shifted relative to those seen in nanovesicles. It is evident from figure 1 that the absorption spectrum of the PDA nanocrystals is qualitatively similar to that of the PDA nanovesicles except

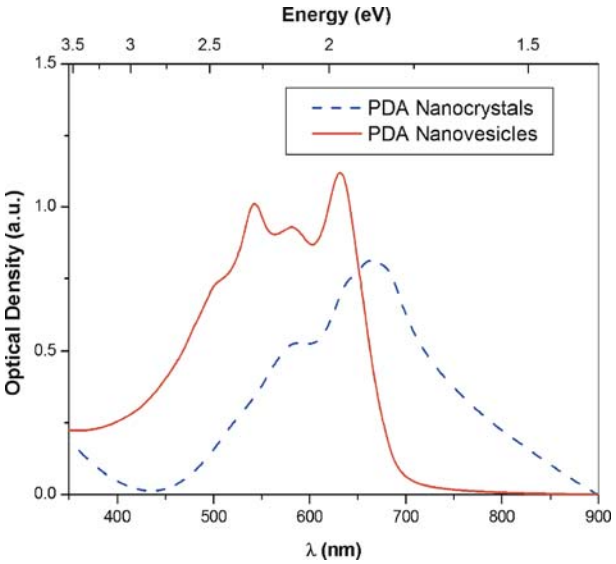

Figure 1. Linear absorption spectra of PDA nanovesicles and PDA nanocrystals.

the peak in between the exciton peak and the corresponding vibronic peak observed in nanovesicles. If this peak was due to the splitting due to chain coupling, then it can be absent in nanocrystals due to different packing of linear array of chains.

UV–Vis absorption spectrum does not reveal the differences between nanoassemblies of polymer chains in nanocrystals and those in nanovesicles. To accomplish this, the microstructure of the PDA nanovesicles and nanocrystals was investigated by transmission electron microscopy (TEM). The TEM image was obtained using Philips CM200 electron microscope. The TEM image of the PDA nanovesicles, shown in figure 2, shows the

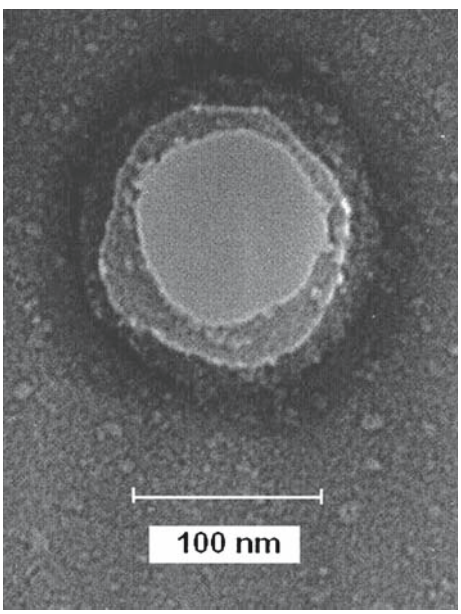

Figure 2. TEM image of PDA nanovesicles.

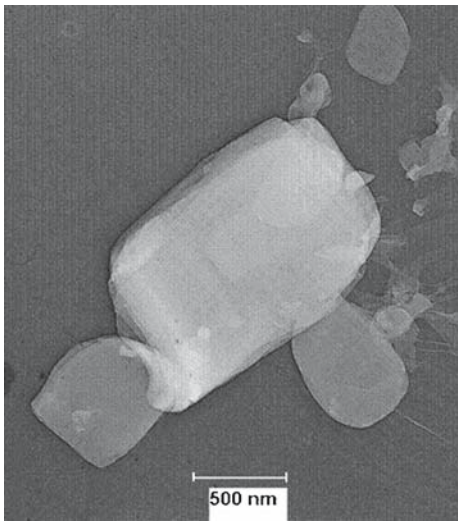

Figure 3. TEM image of PDA nanocrystals.

vesicle shell structure of about 120 nm in diameter. The thickness of the vesicle shell is about 10 nm and the core size is about 100 nm. Figure 3 shows the TEM image of the PDA nanocrystals, with size ranging from 500 nm to 1.5 μm. To ascertain the crystalline nature of the PDA nanocrystals, their TEM diffraction image was also recorded (shown in figure 4). The calculated *d*-spacings obtained from the electron pattern are 2.35 Å, 1.84 Å and 1.37 Å which are similar to that reported in [25]. Poole *et al* [26] have also reported a similar electron diffraction pattern of photo-oxidized polydiacetylene crystals. The TEM picture of the PDA nanovesicles did not show any diffraction fringes, clearly ruling out their crystalline nature.

2.2 *Synthesis and characterization of silver nanoparticles*

Silver nanoparticles were synthesized by following the methodology reported in [27]. An aqueous solution of sodium borohydride (75 ml, 1.2 mM) was taken in a round bottom flask. The flask was put in an ice bath. With continuous stirring of aqueous sodium borohydride solution, an aqueous solution of silver nitrate (9 ml, 2.2 mM) was added drop-wise to it. The resulting solution started changing into golden colour after a few minutes. After mixing the two aqueous solutions, the flask was then removed from the ice bath but the stirring was continued for the next 45 min. Finally the solution was stored under refrigeration.

The silver nanoparticle sample was characterized by transmission electron microscopy (TEM) and UV–Vis absorption spectroscopy. Figure 5 shows the TEM micrograph of the silver nanoparticles. The density of the particles in the TEM picture is sparse, but it contains nanoparticles of different sizes. It can also be seen in the TEM picture that the particles are mostly spherical. Occasional deviation from spherical symmetry, if any, may be attributed to the clustering of the smaller particles upon casting of the sample on the surface of the TEM grid due to the capillary forces. Figure 6 shows the absorption spectrum of the silver nanoparticles in the aqueous solution. The observed absorption spectrum profile is broad and has an asymmetric spanning from 300 nm to 800 nm with a peak at 397 nm. It is very similar to the one reported for an average particle size of ∼25 nm [28]. The inset in figure 6 displays the particles size distribution which shows that the particle size varies from 10 to 100 nm while the peak of the distribution occurs at ∼25–30 nm.

2.3 *Synthesis and characterization of silver nanoparticles-decorated PDA nanovesicles*

For the synthesis of PDA nanovesicles decorated by silver nanoparticles, we used the same monomer, i.e.

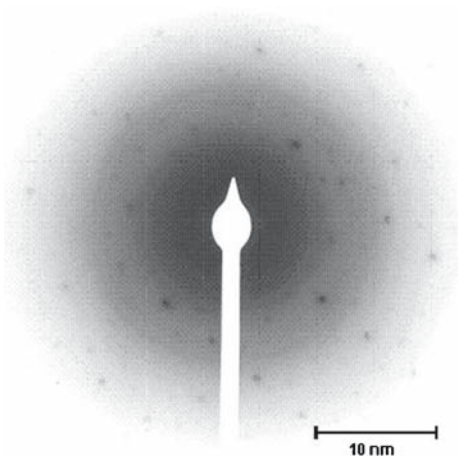

Figure 4. Electron diffraction pattern of PDA nanocrystals.

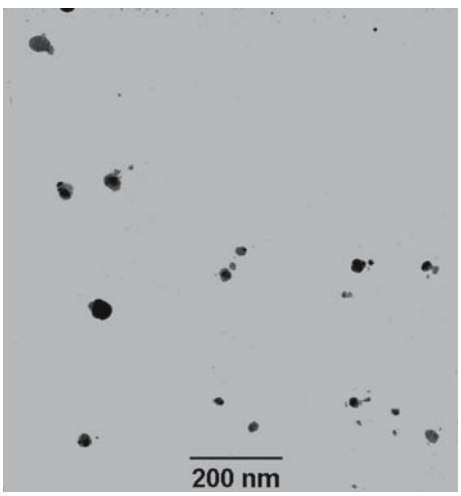

Figure 5. TEM image of silver nanoparticles.

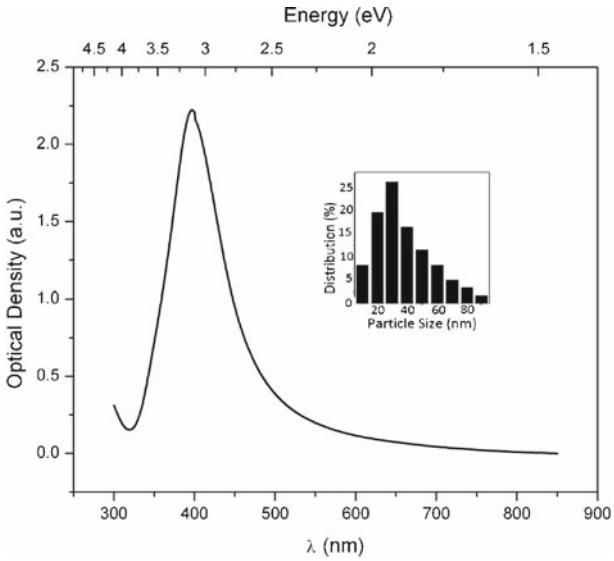

Figure 6. Linear absorption spectrum of silver nanoparticles. The inset shows the particle size distribution.

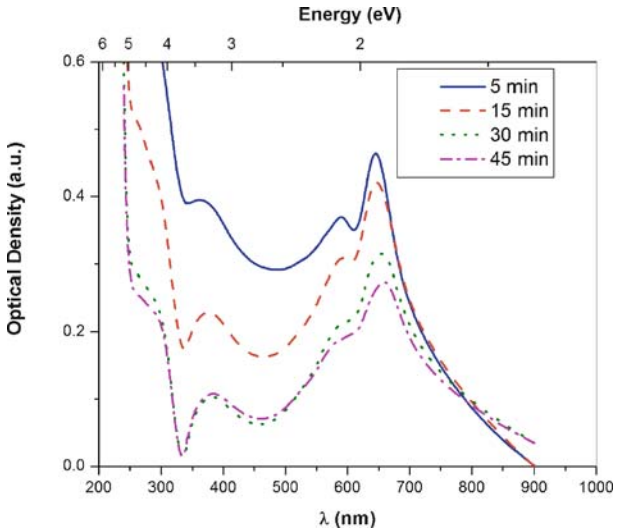

Figure 7. Linear absorption spectra of silver nanoparticles-decorated PDA nanovesicles.

10,12-pentacosadiynoic acid (PCDA), which we used for the synthesis of PDA nanovesicles. A 2 ml volume of 1 mM PCDA solution in ethanol was rotaevaporated to dryness leaving a very thin uniform film of lipid layer on the wall of the flask. Electronic-grade deionized water (15 ml) was then added and heated to 60°C in constant temperature bath while rotating the flask to absolve the lipid layer in water. A 6 ml aqueous solution of $AgNO_3$ of 10^{-2} M concentration was then added to it and the resulting solution was again sonicated in the ultrasonic bath for about 15 min. The semitransparent solution obtained was stored at 4°C in a refrigerator overnight. This solution was then irradiated with UV light (254 nm) for 45 min. For monitoring the growth of silver-coated nanovesicles, UV–Vis absorption spectra was recorded at regular intervals of UV exposure. Figure 7 shows the absorption spectra of the sample after 5, 15, 30 and 45 min of UV exposure. It can be seen that while the optical density (OD) at 265 nm corresponding to the monomer decreases, the peak at 659 nm develops with the exposure of UV radiation. This peak at 659 nm corresponds to the exciton peak of polydiacetylene and its emergence implies the conversion of monomer into polymer. It can also be seen that another peak at 383 nm grows with the increasing dose of UV radiation. This peak corresponds to the surface plasmon band of silver and its growth implies the growth of silver nanoclusters due to photoreduction of Ag ions. The surface plasmon band at 383 nm suggests the diameter of silver nanoparticles to be $<$20 nm [29]. The schemes of polymerization of diacetylene monomers, photoreduction of silver ions and formation of the silver-coated nanovesicles have been explained in detail in ref. [23].

The microstructure of the resulting silver-coated nanovesicles was investigated by transmission electron microscope (TEM) and electron diffraction (ED). The TEM image, displayed in figure 8, shows that the silver-coated PDA nanocomposite sample has a vesicle shell structure with 200 nm outer diameter. The thickness of the vesicle shell is about 20 nm and the core size is about 180 nm. The TEM image reveals the presence of silver nanoparticles on the inner as well as on the outer

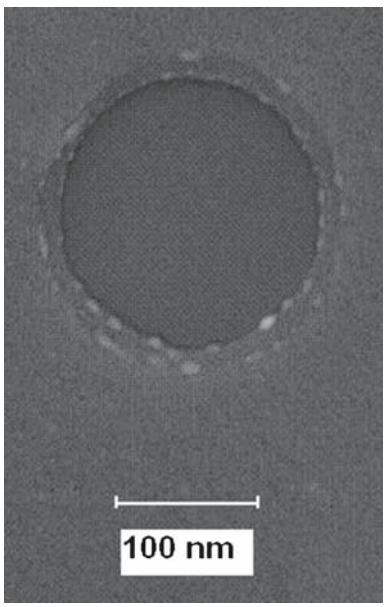

Figure 8. TEM image of silver nanoparticles-decorated PDA nanovesicles.

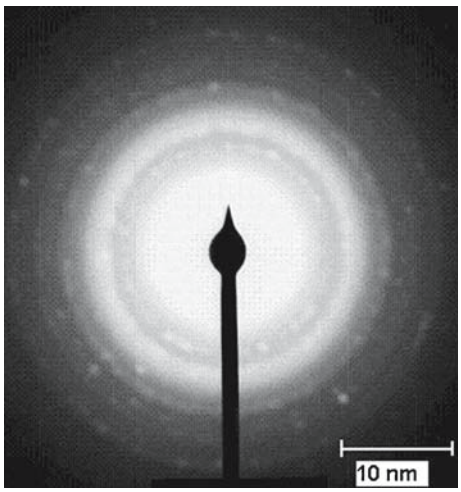

Figure 9. Electron diffraction pattern of silver nanoparticles-decorated PDA nanovesicles.

surfaces of the vesicle. The presence of these silver nanoparticles on the surfaces of the vesicle is further revealed by the ED pattern, displayed in figure 9, which shows four strongest fringes resulting from the diffraction by silver planes [2 2 0], [3 1 1], [3 3 1] and [4 4 0] with plane distances of 1.47 Å, 1.27 Å, 0.94 Å and 0.71 Å respectively.

2.4 *Experimental details*

The third-order nonlinear susceptibility $\chi^{(3)}$ of the samples was measured using antiresonant ring interferometric nonlinear spectroscopic (ARINS) technique [22]. The configuration used for the ARINS set-up is based on the Sagnac interferometer [30]. A typical ARINS experimental set-up is shown in figure 10. This

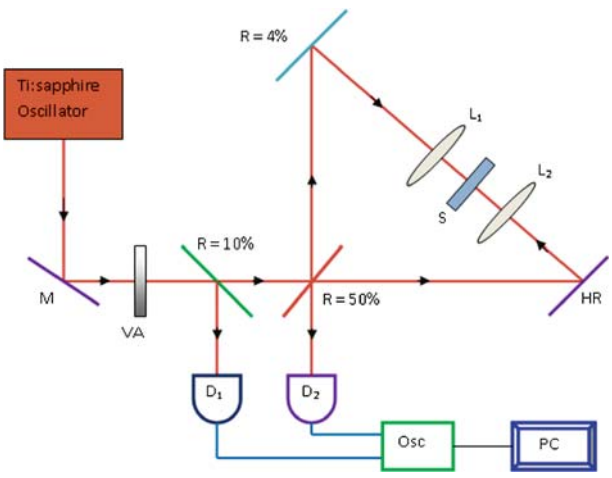

Figure 10. ARINS experimental set-up. M – mirror, L_1, L_2 – lenses, HR – high reflectivity mirror, S – sample, VA – variable attenuator, D_1, D_2 – detectors, Osc – digital oscilloscope, PC – computer.

technique utilizes the dressing of two unequal-intensity counterpropagating pulsed beams with differential nonlinear phases, which occur upon traversing the sample. This difference in phase manifests itself in the intensity-dependent transmission. In this technique, a 50-50 beam splitter divides the incoming pulsed beam into two counterpropagating pulses having a π phase difference. The pulses propagating in the clockwise (CW) direction are reflected by an uncoated flat mirror with wedged rear surface while that propagating in the counterclockwise (CCW) direction are reflected by a high reflectivity mirror. Thus, this technique is based on the dressing of two unequal-intensity counterpropagating pulses. For an exactly 50% beam splitter, in the absence of any nonlinear interactions, the two returning fields will be having the same amplitude but with a phase difference of π between them and consequently they will interfere destructively at the beam splitter to yield zero transmission. Measurement against this dark background provides the basis for the improved sensitivity essential for measuring relatively weak signals. Any small deviation (δ) from the ideal splitting ratio results in a leakage from the ARINS and is responsible for the background illumination that limits the sensitivity of the measurement. If the sample under investigation exhibits nonlinear response, then the two counterpropagating pulses having unequal intensity will undergo different phase changes after passing through the sample. Their superposition on the beam splitter will result in the intensity-dependent transmission of the ARINS which is related to the nonlinear response of the sample. The time difference between the arrivals of the two pulses ($\Delta\tau_{\text{arr}}$) determines the nature of the nonlinear optical process that can be studied depending on its response time. Nonlinear processes with decay time longer than $\Delta\tau_{\text{arr}}$ do not contribute to the intensity- dependent transmission of the ARINS as both the pulses will be affected simultaneously in that case. The delay window thus acts as an ultrafast gate. Hence, this technique has the unique ability to filter the nonresonant electronic contributions from integrating (or slow, e.g. thermal) nonlinearities or those arising from long-lived (resonant) states.

In our investigation of the nonlinear response of the sample, we have used transform-limited, 80 fs pulses (repetition rate = 100 MHz and energy per pulse = 5 nJ) from a self-mode-locked Ti:sapphire laser for the experiment. In order to avoid the contribution of integrating slow nonlinearities and for the measurement of fast electronic nonlinearity only, the sample in a quartz cuvette of 1 mm path length was placed

inside the ring such that the intense pulse arrived earlier at the sample to initiate nonlinear processes, keeping the delay between the intense and weak counterpropagating pulses ≤ 3 ps. Energy of the incident and the transmitted pulses was measured using precalibrated photodetectors. The experimental set-up was standardized using toluene which yielded $n_2 = 6.2 \times 10^{-7}$ cm^2/GW and a negligibly small value of $\beta = 2.5 \times 10^{-3}$ cm/GW corresponding to $\mathrm{Re}\{\chi^{(3)}\} = 3.5 \times 10^{-14}$ esu and $\mathrm{Im}\{\chi^{(3)}\} = 8.8 \times 10^{-16}$ esu respectively. This $\mathrm{Re}\{\chi^{(3)}\}$ value of toluene is in excellent agreement with its earlier reported value determined by another nonlinear interferometric technique [31]. Earlier self-focussing studies on toluene have determined the sign of its nonlinearity to be positive [32,33].

The $\chi^{(3)}$ dispersion of the solution and the solvent was studied at various wavelengths in 720–820 nm range and the second molecular hyperpolarizability γ of the solute (except the sample containing silver nanoparticles only), based on a pairwise additive model for noninteracting molecules, was evaluated using [34]

$$\gamma = \frac{\chi^{(3)}_{\mathrm{solution}} - \chi^{(3)}_{\mathrm{solvent}}}{L^4 N_{\mathrm{solute}}}. \quad (1)$$

Here $\chi^{(3)}_{\mathrm{solution}}$ and $\chi^{(3)}_{\mathrm{solvent}}$ are the third-order susceptibility of the solution and the solvent respectively, N_{solute} is the number density of the solute, $L = (n_0^2 + 2)/3$ is the local field factor and n_0 ($\approx$1.49 for toluene) is the refractive index of the solvent. ARINS intensity scan for the solvent (i.e. water) did not show any measurable nonlinearity. Its value for the evaluation of γ was, therefore, taken to be zero for both real as well as imaginary parts.

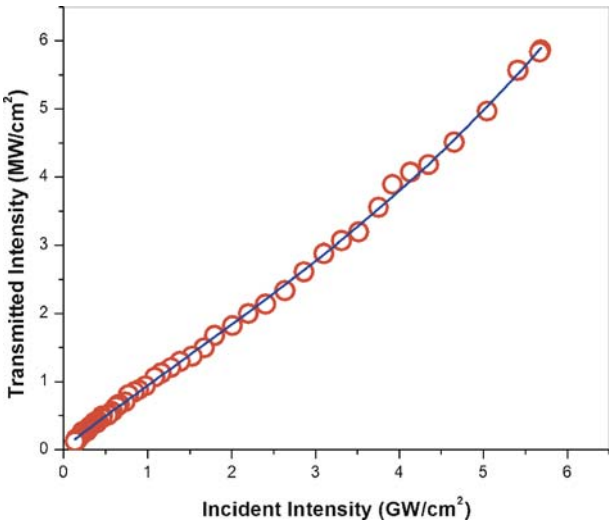

Figure 11. ARINS signal for PDA nanocrystals at 802 nm. Open circles are experimental points. Solid curve is the theoretical fit using the formulation given in ref. [22]. Fit parameters are $\delta = -0.01$, $\beta = 0.11$ cm/GW, $n_2 = 2.43 \times 10^{-6}$ cm^2/GW.

3. Results and discussion

A typical ARINS scan of one of our samples, PDA nanocrystals, at $\lambda = 802$ nm is shown in figure 11. Solid curve is the theoretical fit to the experimental data using the theoretical formalism given in ref. [22]. The fitted values of nonlinear absorption coefficient and nonlinear refractive index are found to be $\beta = 0.11$ cm/GW and $n_2 = 2.43 \times 10^{-6}$ cm^2/GW respectively. From these values of n_2 and β, we calculated the magnitude of the real and imaginary parts of $\chi^{(3)}$ and then subsequently the second molecular hyperpolarizability per unit monomer unit (γ/N) was estimated using eq. (1). The same procedure was followed for PDA nanovesicles and silver nanoparticles-decorated PDA nanovesicles. The measured γ/N values of these three samples in the spectral range of 720–820 nm are shown in figures 12, 13 and 14 respectively. An inspection of the imaginary part of the nonlinearity reveals that as one scans the interrogating wavelength away from one-photon resonance, i.e. from 720 nm to 820 nm, magnitude of the imaginary part of the nonlinearity first decreases and then increases. On the other hand, variation of the real part is rather flat in the observed spectral region. This observed dispersion of the real and imaginary parts of γ/N can be described in the framework of essential states model, according to which nonlinear optical response could be adequately explained by considering only the low-lying three or four states [35–37].

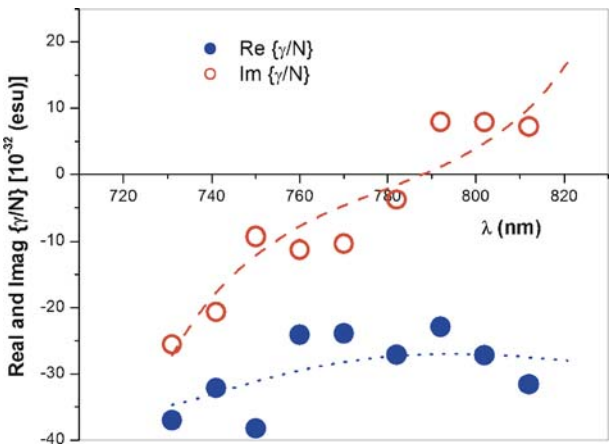

Figure 12. Three-essential states model fit to the dispersion of the real and imaginary parts of γ/N of PDA nanocrystals. Solid circles and open circles are the experimental points of $\mathrm{Re}\{\gamma/N\}$ and $\mathrm{Im}\{\gamma/N\}$ respectively. Dotted line and dashed line are their respective theoretical fits.

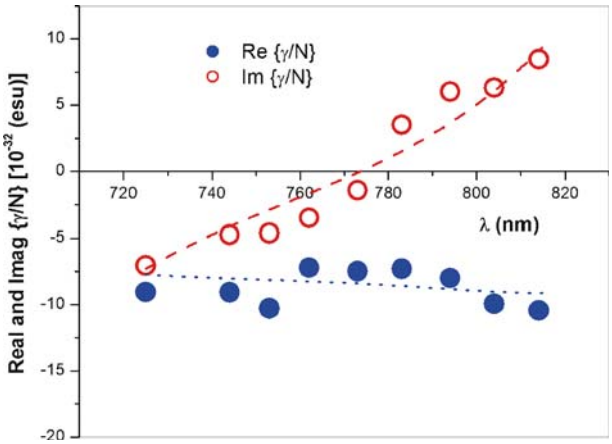

Figure 13. Three-essential states model fit to the dispersion of the real and imaginary parts of γ/N of uncoated PDA nanovesicles. Solid circles and open circles are the experimental points of $\mathrm{Re}\{\gamma/N\}$ and $\mathrm{Im}\{\gamma/N\}$ respectively. Dotted line and dashed line are their respective theoretical fits.

In the three-level model, these have been identified as the ground state $|0\rangle$ and the lowest one- and two-photon allowed states $|1\rangle$ and $|2\rangle$ respectively. According to the perturbation expansion given by Orr and Ward [38], the second molecular hyperpolarizability in this case is given by

$$\gamma(\omega_\sigma;\omega_1,\omega_2,\omega_3) = aK\hbar^{-3}\mu_{01}^4\left[\left(\frac{\mu_{12}}{\mu_{01}}\right)^2 T_{121} + \left(\frac{\Delta\mu}{\mu_{01}}\right)^2 T_{111} - D_{11}\right], \quad (2)$$

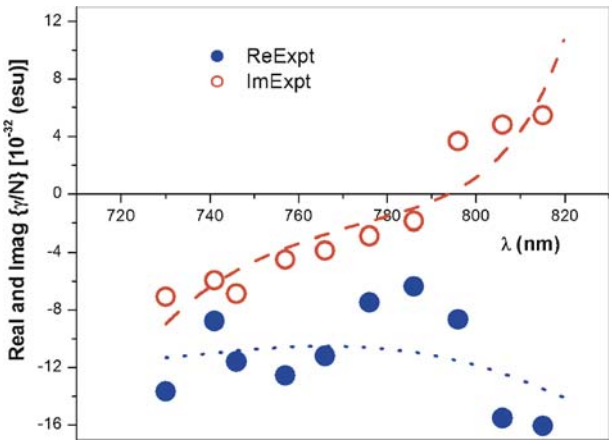

Figure 14. Three-essential states model fit to the dispersion of the real and imaginary parts of γ/N of silver nanoparticles-coated PDA nanovesicles. Solid circles and open circles are the experimental points of $\mathrm{Re}\{\gamma/N\}$ and $\mathrm{Im}\{\gamma/N\}$ respectively. Dotted line and dashed line are their respective theoretical fits.

where K is a constant that depends on the frequency and degeneracy of a given optical process, μ_{lm} is the electronic transition dipole moment between states $|l\rangle$ and $|m\rangle$, $\Delta\mu = \mu_{11} - \mu_{00}$ is the dipole difference, ω_1, ω_2, ω_3 are the frequencies of the perturbing radiation fields, $\omega_\sigma = \omega_1 + \omega_2 + \omega_3$ is the polarization response frequency while a indicates the orientational average which is 1/5 for an isotropic liquid. For self-action process presented in this paper, $\omega_1 = \omega_2 = -\omega_3 = \omega$. The expressions T_{121} and D_{11} represent the contributions from the two-photon and one-photon transition channels respectively while T_{111} is nonzero only for noncentrosymmetric structures [39].

We have pointed out above that as the interrogating wavelength moves away from one-photon resonance i.e. from 720 to 820 nm, the magnitude of the imaginary part of the nonlinearity first decreases and then increases. On the other hand, variation of the real part is rather flat in the observed spectral region. Such a scenario is indeed anticipated in three-essential states model when one- and two-photon channels are placed with respect to the spectral region of interest (photon energies of the exciting radiation) such that their respective negative and positive contributions to the imaginary parts of the nonlinearity interfere destructively, i.e. mutually cancel each other partially and their contributions to the real part reinforce each other to yield its rather flat dispersion. As the one-photon channel contribution below resonance, as is the case here, will always be negative, its reinforcement by two-photon channel would mean a negative contribution from this channel as well. This would imply that the two-photon energy of excitation radiation is larger than the transition energy of the two-photon channel over the entire spectral region addressed in our experiments. Considering the fact that a two-photon allowed energy state 2^1A_g has been observed lying above one-photon state ^1B_u at ~2.85 eV in polydiacetylenes [7] and one-photon allowed state in our sample is located above the higher energy end of the spectral range of investigation (1.72–1.51 eV), the above-mentioned situation is indeed applicable here. We, therefore, consider the three-essential states model for the quantitative description of our experimentally observed spectral dispersion characteristic of second molecular hyperpolarizability. The respective sign of $\mathrm{Re}\{\gamma/N\}$ and $\mathrm{Im}\{\gamma/N\}$ has been assigned commensurate with the above discussion.

As the photon energies in our spectral range of investigation are near resonance with the two channels, the dominant terms in the expression of three-essential

states model of γ given by eq. (2) will alone suffice. The resulting expression for γ/N is then given by [40]

$$\left\{\frac{\gamma}{N}\right\} = \frac{|\mu_{10}|^2}{(\Omega_{10}-\omega)^2}\left\{\frac{|\mu_{12}|^2}{(\Omega_{20}-2\omega)} - \frac{|\mu_{10}|^2}{(\Omega_{10}-\omega)}\right\} + \frac{|\mu_{10}|^2}{(\Omega_{10}-\omega)(\Omega_{10}^*-\omega)} \times \left\{\frac{|\mu_{12}|^2}{(\Omega_{20}-2\omega)} - \frac{|\mu_{10}|^2}{(\Omega_{10}-\omega)}\right\}. \quad (3)$$

Resulting fits to the experimental dispersion of $\mathrm{Re}\{\gamma/N\}$ and $\mathrm{Im}\{\gamma/N\}$ for PDA samples are shown in figures 12, 13 and 14. It can be seen from these figures that the three-essential states model provides satisfactory description of the observed dispersion of γ/N for the three PDA samples. We have shown the values of the best-fit parameters for the three PDA samples in table 1. It can be seen that the two-photon state in PDA nanocrystals as well as in PDA nanovesicles occurs at nearly the same energy (∼2.85 eV), a value which is in excellent agreement with the earlier reported value for the two-photon state energy in polydiacetylene [7]. Slightly higher values of transition dipole moments μ_{01} and μ_{12} as well as of the ratio μ_{12}/μ_{01} are predicted for nanocrystals. Polymer chains are relatively more strained in the case of nanovesicles due to the positive outward pressure. This may be partly responsible for the differences in their properties of electronic structure. Higher transition moments in conjunction with the lower energy for the one-photon state in nanocrystals by ∼0.1 eV are responsible for the higher negative value of nonlinearity at shorter wavelengths in nanocrystals. It would be very interesting to compare the best-fit parameters of the silver-coated nanovesicles with that of uncoated (bare) PDA nanovesicles. The observed one-photon state in bare nanovesicles occurs at 1.97 eV, which is higher than that observed in coated nanovesicles by 0.09 eV. However, in coated nanovesicles, the two-photon state is observed to lie at a slightly higher value (∼2.92 eV). Therefore, our observation reveals that compared to bare nanovesicles, the decoration of silver nanoparticles shifts the one-photon state of the composite system to lower energy while that of the two-photon state to higher energy. Our analysis also suggests lower μ_{01} and higher μ_{12} values for coated vesicles than that observed in bare vesicles. The predicted difference in the property of the electronic structure of coated nanovesicles compared to that of bare nanovesicles implies a definite coupling between free electrons of the metal and π electrons of the polymer. This coupling was confirmed when we investigated the third-order nonlinear optical response of silver nanoparticles in aqueous solution over the same spectral range (720–820 nm), the results of which have been published by our group elsewhere [41]. The observed spectral dispersion of the real and imaginary parts of nonlinearity for the silver nanoparticles is shown in figure 15. From this figure, we observe that the spectral dispersion of the real and imaginary parts of nonlinearity for the silver nanoparticles did not show any resemblance to the spectral dispersion characteristics shown by silver nanoparticles-decorated PDA nanovesicles (shown in figure 14). On the other hand, the spectral dispersion of γ for coated nanovesicles is very much similar to that of bare nanovesicles (shown in figure 13). However, the values of γ for coated nanovesicles are slightly higher than that of bare nanovesicles. This suggests that the spectral dispersion of γ for coated nanovesicles is predominantly due to PDA, with only a slight increase in γ values because of the presence of silver nanoparticles as a result of enhanced local electromagnetic field due to SPR. The slight increase in γ values for coated nanovesicles, therefore, implies a weak coupling between π electrons of the polymer and free electrons of silver nanoparticles in the composite system.

Comparing the values of $\mathrm{Re}\{\gamma/N\}$ and $\mathrm{Im}\{\gamma/N\}$ as shown in figures 12, 13 and 14, we see that the PDA nanocrystals exhibit nonlinearities higher than the values exhibited by PDA nanovesicles as well as PDA nanovesicles decorated by silver nanoparticles. Here, we are offering a plausible explanation

Table 1. Best-fit parameters (location of the excited states, their linewidths and transition dipole moments between them) for PDA nanocrystals, uncoated PDA nanovesicles and coated PDA nanovesicles used in the three-essential states model.

Sample	E_{01} (Obs.) (eV/nm)	Γ_{01} (eV)	E_{02} (eV)	Γ_{02} (eV)	μ_{01} (D)	μ_{12} (D)
PDA nanocrystals	1.87/664	0.06	2.85	0.06	12.96	48.29
Uncoated PDA nanovesicles	1.97/631	0.10	2.86	0.10	11.57	42.77
Coated PDA nanovesicles	1.88/659	0.07	2.92	0.04	8.78	43.15

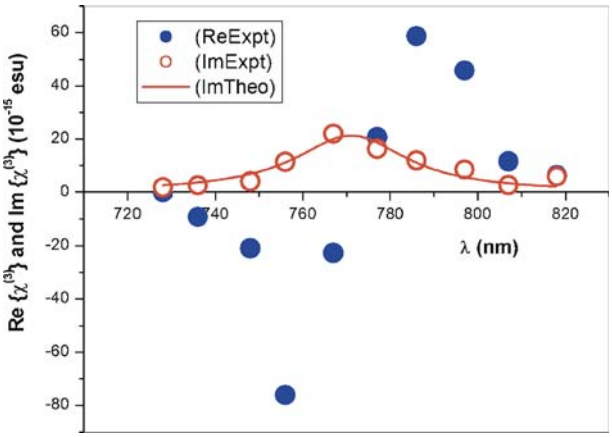

Figure 15. Spectral dispersion of Re$\{\chi^{(3)}\}$ and Im$\{\chi^{(3)}\}$ of Ag nanoparticles. Solid circles and open circles are experimental points of Re$\{\chi^{(3)}\}$ and Im$\{\chi^{(3)}\}$ respectively. Solid curve is the theoretical fit to the experimental points of Im$\{\chi^{(3)}\}$ using the formulation given in ref. [42].

for the enhancement of nonlinearity in PDA nanocrystals. We have already stated that the diffraction fringes in the TEM picture of PDA nanocrystals confirm their crystalline nature, indicating that the nanocrystals have orderly arrangement of conjugated polymer chains. It has been observed that in conjugated molecules, the cubic hyperpolarizability increases very rapidly with molecular dimensions according to a power law as against that in saturated molecules with the same number of valence electrons [42]. According to the free electron model of Rustagi and Ducuing, the cubic hyperpolarizability of π-conjugated molecules scales as the fifth power of the chain length [43]. Agrawal *et al* calculated γ for polydiacetylenes in the tight binding approximation and predicted the sixth power dependence on the chain length [44]. As PDA nanocrystals have orderly arrangement of polymer chains, the enhancement in their nonlinearity is proportional to their chain length. On the other hand, the TEM picture of nanovesicles did not show any diffraction fringes and thus their crystalline nature was ruled out. This is further substantiated by the presence of the third peak between the exciton peak and the vibronic peak in uncoated nanovesicles, compared to that of nanocrystals. We have inferred above that the presence of this peak in nanovesicles might be because of the splitting of chain coupling, thus preventing them from having an ordered set of polymer chains. Moreover, the strain on the polymer chains due to the positive outward pressure in nanovesicles may also be contributing in disrupting the chains from making an ordered array of chains and thereby showing lower values of cubic hyperpolarizability. We can, therefore, infer that the arrangement of polymer chains in PDA nanocrystals is more favourable for higher nonlinearity.

As stated above, contrary to our expectation that the presence of silver nanoparticles on PDA nanovesicles could enhance the nonlinearity of the composite system considerably, our investigation revealed only a weak coupling between π electrons of the polymer and free electrons of the silver nanoparticles. One of the probable reasons for this weak coupling could be our measurement of nonlinear properties in the spectral range of 720–820 nm, which is quite far from the plasmon frequency of the silver nanoparticles (observed at ~383 nm) as well as 1D exciton frequency of the polymer (observed at ~659 nm). We conjecture that gold-coated PDA vesicles may be more rewarding due to the stronger coupling expected between free electrons of gold nanoparticles and π electrons of the polymer as the plasmon frequency of gold nanoparticles (~530 nm) is nearer to the exciton frequency of PDA (~659 nm). Another interesting exploration could be controlling the shape and size of nanoparticles decorating the PDA nanovesicles thereby changing the electronic structure of the nanocomposite to favour higher nonlinearity. We hope that further research in this direction may result in better understanding of the coupling between π electrons of the polymer and free electrons of the metal nanoparticles in the case of polymer–metal nanoparticle composite systems, which may lead to the development of novel, efficient and tunable nonlinear optical materials with large third-order nonlinear susceptibility.

4. Conclusions

Our paper reports the synthesis, characterization and investigation of third-order nonlinear optical properties of two different nanostructures of PDA, namely PDA nanocrystals and PDA nanovesicles, along with PDA nanovesicles decorated by silver nanoparticles. The third-order nonlinear susceptibility was measured by antiresonant ring interferometric nonlinear spectroscopic (ARINS) technique using the femtosecond mode-locked Ti:sapphire laser in the spectral range of 720–820 nm. Our investigation has revealed the influence of chain coupling effects facilitated by the chain packing geometry of PDAs on their third-order optical nonlinearity. We found that the linear arrangement of polymer chains in PDA nanocrystals favours high nonlinearity. The presence of silver nanoparticles increases the γ values of PDA–silver nanocomposites

only slightly because of the surface plasmon resonance of nanoparticles, suggesting a weak coupling between free electrons of the metal and π electrons of the polymer. The spectral dispersion characteristic of γ for silver nanoparticles-coated PDA nanovesicles is found to be qualitatively similar to that observed for uncoated PDA nanovesicles but bears no resemblance to that observed in silver nanoparticles. The observed spectral dispersion of γ has been explained in the framework of three-essential states model and a correlation between the electronic structure and optical nonlinearity of the samples has been established. We have also suggested some ways to enhance the optical nonlinearity of polymer–metal nanocomposites, which may lead to the development of novel, efficient and tunable nonlinear optical materials with large third-order nonlinear susceptibility.

Acknowledgement

The corresponding author acknowledges the financial support for this research work by the University Grants Commission (UGC), Government of India (CSIR-UGC Research Fellowship, F. No. 2-44/2000(i)-EU II dated 1.2.2001).

References

[1] M G Kuzyk, *Phys. Rev. Lett.* **85**, 1218 (2000)
[2] B Bhushan, S K Kumar, S S Talwar, T Kundu and B P Singh, *Appl. Phys. B* **109**, 201 (2012)
[3] J C May, I Biaggio, F Bures and F Diederich, *Appl. Phys. Lett.* **90**, 251106 (2007)
[4] C Sauteret, J P Hermann, R Frey, F Pradere, J Ducuing, R H Baughman and R R Chance, *Phys. Rev. Lett.* **36**, 956 (1976)
[5] J Bolger, T G Harvey, W Ji, A K Kar, S Molyneux, B S Wherrett, D Bloor and P Norman, *J. Opt. Soc. Am. B* **9**, 1552 (1992)
[6] G M Carter, J V Hryniewicz, M K Thakur, Y J Chen and S E Meyler, *Appl. Phys. Lett.* **49**, 998 (1986)
[7] G Banfi, D Fortusini, P Dainesi, D Grando and S Sottini, *J. Chem. Phys.* **108**, 4319 (1998)
[8] B Bhushan, T Kundu and B P Singh, *Opt. Photon. J.* **3**, 278 (2013)
[9] D Ricard, P Roussignol and C Flytzanis, *Opt. Lett.* **10**, 511 (1985)
[10] M J Bloemer, J W Haus and P R Ashley, *J. Opt. Soc. Am. B* **7**, 790 (1990)
[11] S Lysenko, J Jimenez, G Zhang and H Liu, *J. Electron. Mater.* **35**, 1715 (2006)
[12] F Hache, D Ricard and C Flytzanis, *J. Opt. Soc. Am. B* **3**, 1647 (1986)
[13] K Uchida, S Kaneko, S Omi, C Hata, H Tanji, Y Asahara, A J Ikushima, T Tokisaki and A Nakamura, *J. Opt. Soc. Am. B* **11**, 1236 (1994)
[14] C Voisin, N D Fatti, D Christofilos and F Vallee, *J. Phys. Chem. B* **105**, 2264 (2001)
[15] A E Neeves and M H Birnboim, *J. Opt. Soc. Am. B* **6**, 787 (1989)
[16] N Kalyaniwalla, J W Haus, R Inguva and M H Birnboim, *Phys. Rev. A* **42**, 5613 (1990)
[17] J W Haus, H S Zhou, S Takami, M Hirasawa, I Honma and H Komiyama, *J. Appl. Phys.* **73**, 1043 (1993)
[18] J Tao, H Jiang, J Wang, G Zou and Q Zhang, *Chem. Phys. Lett.* **539–540**, 70 (2012)
[19] X Chen, J Tao, G Zou, W Su, Q Zhang and P Wang, *Curr. Nanosci.* **7**, 556 (2011)
[20] X Chen, J Tao, G Zou, W Su, Q Zhang and P Wang, *Chem. Phys. Chem.* **11**, 3599 (2010)
[21] X Chen, G Zou, Y Deng and Q Zhang, *Nanotechnol.* **19**, 195703 (2008)
[22] P Vasa, B P Singh, P Taneja and P Ayyub, *Opt. Commun.* **233**, 297 (2004)
[23] H S Zhou, T Wada, H Sasabe and H Komiyama, *Synth. Metals* **81**, 129 (1996)
[24] E K Ji, D J Ahn and J M Kim, *Bull. Kor. Chem. Soc.* **24**, 667 (2003)
[25] R J Young, R T Read, D Bloor and D Ando, *Faraday Dis. Chem. Soc.* **68**, 509 (1979)
[26] N J Poole, B J E Smith, D N Batchelder, R T Read and R J Young, *J. Mater. Sci.* **21**, 507 (1986)
[27] R Keir, D Sadler and W E Smith, *Appl. Spectrosc.* **56**, 551 (2002)
[28] Y Zhao, Y Ziang and Y Fang, *Spectrochim. Acta Part A* **65**, 1003 (2006)
[29] J Yguerabide and E E Yguerabide, *Anal. Biochem.* **262**, 137 (1998)
[30] M C Gabriel, N A Whitaker Jr, C W Dirk, M G Kuzyk and M Thakur, *Opt. Lett.* **16**, 1334 (1991)
[31] N P Xuan, J L Ferrier, J Gazengel and G Rivoire, *Opt. Commun.* **51**, 433 (1984)
[32] G Rivoire, C Deslancs, J L Ferrier, J Gazengel and N P Xuan, *Opt. Quant. Elect.* **15**, 209 (1983)
[33] J Gazengel and G Rivoire, *Opt. Acta* **26**, 483 (1979)
[34] M T Zhao, M Samoc, B P Singh and P N Prasad, *J. Phys. Chem.* **93**, 7916 (1989)
[35] D Guo, S Mazumdar, S N Dixit, F Kajzar, F Jarka, Y Kawabe and N Peyghambarian, *Phys. Rev. B* **48**, 1433 (1993)
[36] J W Wu, J R Heflin, R A Norwood, K Y Wong, O Zamani-Khamiri, A F Garito, P Kalyanaraman and J Sounik, *J. Opt. Soc. Am. B* **6**, 707 (1989)
[37] C W Dirk, L T Cheng and M G Kuzyk, *Int. J. Quantum Chem.* **43**, 27 (1992)
[38] B J Orr and J F Ward, *Mol. Phys.* **20**, 513 (1971)
[39] A V V Nampoothiri, P N Puntambekar, B P Singh, R Sachdeva, A Sarkar, D Saha, A N Suresh and S S Talwar, *J. Chem. Phys.* **109**, 685 (1998)
[40] B Bhushan, T Kundu and B P Singh, *Opt. Commun.* **312**, 127 (2014)
[41] B Bhushan, T Kundu and B P Singh, *Opt. Commun.* **285**, 5420 (2012)
[42] J P Hermann and J Ducuing, *J. Appl. Phys.* **45**, 5100 (1974)
[43] K C Rustagi and J Ducuing, *Opt. Commun.* **10**, 258 (1974)
[44] G P Agrawal, C Cojan and C Flytzanis, *Phys. Rev. B* **17**, 776 (1978)